

Reservoir Characterization using Simultaneous Inversion, AVO Analysis, and Seismic Attributes: A Case Study of Conglomerates-Volcanic, Northwest Java Basin

Saeful Ghofar Zamianie Putra¹, Muhammad Oktama Aulia Akbar²,
Putra Pratama Wahyu Hidayat², Sudarmaji Saroji³, Sismanto Sismanto^{3,*}

¹Physics Department, Gadjah Mada University, Sekip Utara, Bulaksumur, Yogyakarta 55281, Indonesia

²PT. Pertamina EP, Cirebon, West Java, Indonesia

³Geophysics Laboratory, Physics Department, Gadjah Mada University, Sekip Utara, Bulaksumur, Yogyakarta 55281, Indonesia

*Author to whom correspondence should be addressed:
E-mail: sismanto@ugm.ac.id

(Received February 06, 2025; Revised August 27, 2025; Accepted November 12, 2025)

Abstract: The Northwest Java Basin (NWJB) in Indonesia is a productive basin with proven oil and gas production. It consists of conglomerate, volcanic rock, and shale. A key exploration challenge in the NWJB is the extensive volcanic cover, which significantly reduces the effectiveness of conventional seismic methods. In this study, we employ seismic interpretation techniques to address these challenges and enhance the success of oil and gas exploration in volcanic-dominated settings. This study uses simultaneous inversion to characterize conglomerate distribution among volcanic rocks, using sensitive parameters like V_p/V_s , density, and lambda-rho. The study also uses AVO analysis on the LAC-12 well to identify potential locations. The study uses RMS amplitude, sweetness, and spectral decomposition attributes to support the structure at the study site. The simultaneous inversion was proven to characterize the distribution of conglomerate among volcanic rocks by using several sensitive parameters consisting of V_p/V_s with a cut-off value of <1.6 , density with a cut-off value of <2.35 g/cc, and lambda-rho, or incompressibility, <20 Gpa*g/cc. Furthermore, AVO analysis on the LAC-12 well showed that the reservoir in this study was of class IIP AVO type at the top and class II at the base. These attributes are integrated with the inversion parameter and supported by the interpretation of the AVO attribute cross-section, which produces three potential locations in the pre-TAF horizon with a depth of about 2100 ms.

Keywords: attribute AVO; conglomerate distribution; lambda-rho; Northwest Java Basin; Pre-TAF; volcanic rocks

1. Introduction

According to SKK Miga's annual report, of the 128 basins located in Indonesia, there are 68 yet to be explored. This happens because of the high number of risks associated with the failure of exploration projects and the high cost of exploration since Indonesia is an archipelago, which makes the cost even higher in remote areas such as the as the east part of Indonesia. Furthermore, the exploration of new potential in development areas is increased by the government through contractor companies in Indonesia. In those areas, maximizing mature fields or basins can significantly increase production. Through many basins in Indonesia, the Northwest Java basin is the one that has

consistently produced oil and gas since 1939 at Randegan. The Northwest Java Basin (NWJB) is one of the most productive basins with proven oil and gas production¹⁾. NWJB is a basin formed of half-graben that is in the south end of Sunda land in Tertiary time. This basin covers the northern part of West Java until the offshore area reaches the south of Sumatera Island (Figure 1)²⁾. The USGS estimated there are 2008 billion barrels of oil equivalent (BOE), 658 million barrels of oil, 7453 mmscf of gas, and 108 million LNG potentials³⁾. Tectonically, the NWJB basin (Figure 1.A) is formed due to a rifting process followed by subduction that creates several major structures. While stratigraphically, this basin consists of several formations, namely: the Basement,

composed of igneous and metamorphic rocks; the Jatibarang Formation, composed of tuff, breccia, and extrusive rock; the Talang Akar Formation, composed of alternating tuff and conglomerate at the beginning, then alternating sandstone and shale, and ending with alternating sandstone, shale, and carbonate rock; the Baturaja Formation, which is mostly composed of carbonate rocks; the Upper Cibulakan, composed of sandstone, carbonate, and shale; the Parigi Formation, composed of carbonate rocks and shale; and lastly, the Cisubuh Formation, which is mostly composed of shale as cap rock in this basin (Figure 1.B)^{4,5}. Several formations have been actively produced, such as Talang Akar, Baturaja, Upper Cibulakan, and Parigi. However, there is one potential location that has not been exploited, which is the Pre-Talang Akar Formation (Pre-TAF), which is located between Jatibarang and the Talang Akar Formation⁴. Pre-TAF consists of conglomerate, volcanic rock such as tuff and breccia, and shale. One of the challenges in exploring this formation is the presence of dominant volcanic coverage among conglomerate rock, which is a potential reservoir rock⁶. As we know, volcanic coverage on the subsurface remains one challenge that hinders the exploration of oil and gas using seismic methods. The seismic method is incompatible with use in volcanic lithologies because of the complex and heterogeneous structure that volcanic lithologies have, with variable porosity and permeability. This heterogeneity can cause variations in seismic velocities and anisotropic behavior, making the seismic response more complex and challenging to interpret accurately. To overcome the interpretation challenges in the Pre-Talang Akar Formation (Pre-TAF), this study will conduct seismic interpretation using simultaneous inversion, Avo analysis and seismic attributes to characterize conglomerate distribution among volcanic rocks.

There are many ways to interpret seismic data⁷; however,

one of the most common and proven techniques is interpreting pre-stack seismic data. Using pre-stack seismic data has several advantages, including better resolution and complete data (angle and offset information). To use pre-stack seismic data to the fullest, seismic inversion and amplitude variation by offset (AVO) analysis are a couple of ways to interpret pre-stack seismic data. Simultaneous inversion is a method to quantify subsurface parameters by inverting seismic trace data into impedances and density. The other is AVO analysis, which analyzes the change in amplitude as the offset or angle increases^{8,9}. This change in amplitude contains valuable information that we can categorize into several types^{10,11}. Finally, with the help of seismic attributes from post-stack seismic data, we can extract additional information that could support our previous interpretation, including structural and geometrical characteristics, the distribution of sandstone, and even reservoir potential^{12,13}.

Pre-TAF remains understudied and explored, with few comprehensive geophysics research publications related to hydrocarbon exploration. A recent study about this interval was in South Sumatra in Jabung Block¹⁴. This study is AVO analysis in the pre-TAF interval. They conclude that this interval has AVO type II, which is a low-impedance sandstone. Furthermore, they used the AVO P*G attribute to see the distribution of the reservoir compared to the Lower Talang Akar Formation (LTAF), which is already producing oil and gas in Jabung Block. The AVO attribute shows a good correlation between pre-TAF and LTAF reservoir distribution, and they have the same class of AVO, which is AVO class II¹⁴. This study mainly focuses on characterizing Pre-TAF (Figure 1.B) and Northwest Java Basin reservoir potential by interpreting seismic data using two methods: simultaneous inversion, AVO analysis, and seismic attributes. This study aims to provide a better understanding and suggestions for new potential reservoirs to drill.

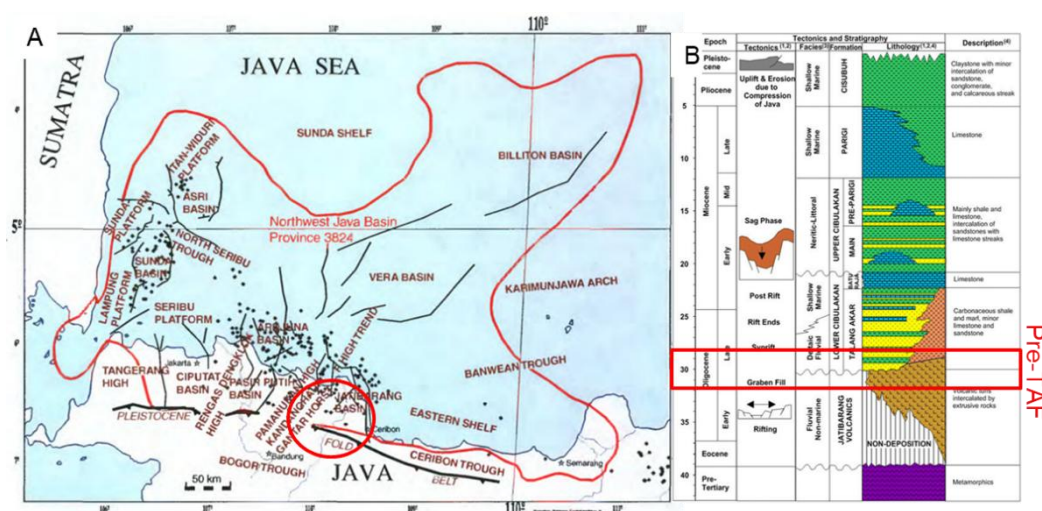


Fig. 1: The Northwest Java basin lies over North Java to South Sumatera², and the study area is located around within the red circle (A) Tectonics and (B) stratigraphic column for NWJB and the interval of interest at Pre-Talang Akar Formation⁴

2. Materials and method

In this study, five wells are used for all the processes that contain several important logs, including logs that were acquired from petrophysics analysis such as effective porosity (PHIE), saturation water (SWT), and volume of shale (Vshale). In all five wells in this study, only two wells have check shot measurements in wells LAL-18 and LAC-20, and only one well with the shear wave (Vs) log is available in well LAC-12. The two check shots were applied to each nearest remaining well for check shot correction, and the wavelet that was used is a statistical wavelet extracted from full-stack seismic data (Figure 2). Well, seismic ties were conducted on all the wells to obtain full-stack seismic data, which resulted in a good correlation from all wells above 0.5¹⁵⁾. The next step is picking the horizon and structure step in the seismic data. There were two horizons created, which are Pre-TAF and Top Basement. Since the Vs log was not available in four other wells, synthetic Vs logs were generated using the Xu-White method¹⁶⁾, employing the volume of shale as input for mineral constraint, saturation water as saturation in situ, and RHOB and PHIE as the density and porosity models^{14,15)}. The Xu-White method was selected as it demonstrates the highest correlation between the estimated Vs and the measured Vs in well LAC-12, outperforming the other methods (Table 1).

Furthermore, sensitivity analysis was performed by cross-posting inversion parameters with several logs, like volume of shale, triple combo logs, etc. Two kinds of seismic data were used in this research. The first is the pre-stack CDP gather that is used for seismic pre-stack inversion and AVO analysis¹⁷⁾, while the other is full-stack seismic for well seismic tie and horizon picking. The CDP gather underwent pre-conditioning of traces that followed the procedure from Maurya, starting with filtering until angle gather conversion¹⁵⁾. The workflow of reservoir characterization in this study shows in Figure 3.

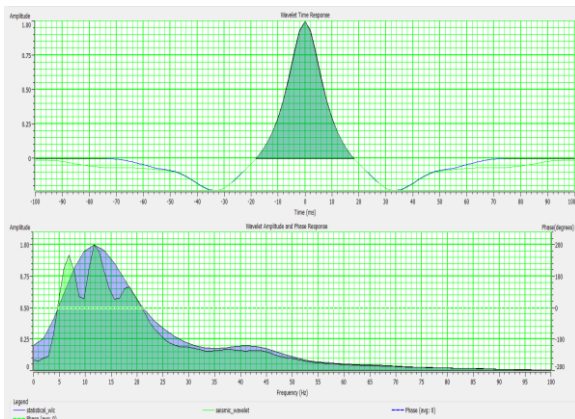


Fig. 2: Statistical wavelet extracted from full-stack seismic data and the comparison between the extracted statistical wavelet and seismic spectral analysis

Table 1: Comparison of the Vs log with the synthetic vs using different method in well LAC-12

Method	Cross Correlation
Castagna	-0.0166
Krief	-0.0058
Greenberg-Castagna	0.3371
Xu-White	0.5442

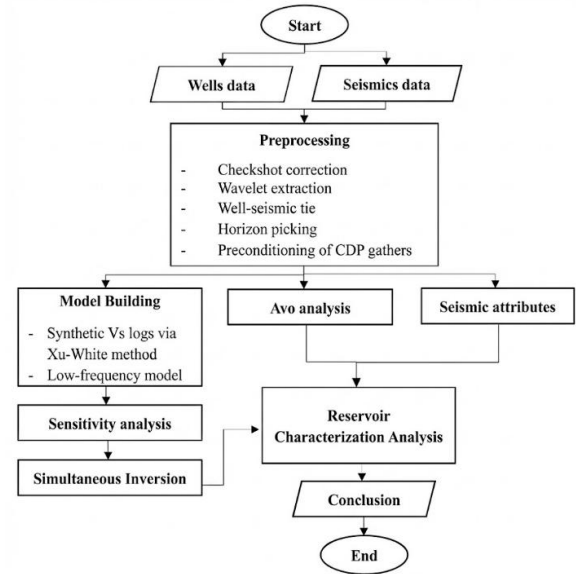


Fig. 3: The workflow of reservoir characterization in this study

Two horizons were used to build low-frequency models before the pre-stack simultaneous inversion. Next, we extract statistical wavelets from our angle and gather seismic data that is divided into three angles: near angle 0–12, mid angle 13–22, and far angle 23–35. The inversion analysis uses the Fatti approximation^{17,18,19)}

$$R_{PP}(\theta) = 1 + \tan^2 \theta R_{P0} + 8 \left(\frac{V_s}{V_p} \right)^2 \sin^2 \theta R_{S0} + \frac{1}{2} \left[\frac{\Delta V_s}{V_s} + \frac{\Delta \rho}{\rho} \right] R_D \quad (1)$$

where R_P is the reflectivity of the p-wave, R_S is the reflectivity of the s-wave, and R_D is the reflectivity of density. The quality control is being done by comparing the inverted log and the original log (Table 2). The correlation of V_p/V_s was found to be very weak, with a coefficient of only 0.171. Therefore, the direct V_p/V_s results were deemed unreliable and subsequently excluded from further analysis. Instead, during the inversion process, the V_p/V_s ratio was derived manually by computing the division of inverted V_p by the inverted V_s .

The linear regression between the acoustic impedance and shear impedance, acoustic impedance, and density was taken, which resulted in certain values k, m, kc, and mc. The gamma value was 0.3 for the background ratio. Furthermore, the pre-whitening method used was covariance, with a pre-whitening value of 10%, and the

Table 2: Presents a comparison between the original well logs and the inverted logs employed as parameters in the simultaneous inversion, which are then propagated throughout the seismic dataset

Parameters	Correlation
Acoustic Impedance	0.787
Shear Impedance	0.777
Density	0.755
Vp	0.755
Vs	0.671
Vp/Vs	0.171

number of iterations was 50 times. Finally, the simultaneous inversion was applied to the angle gathered to obtain the acoustic impedance, shear impedance, density, and P- to S-wave velocity ratio cube/volumes. AVO analysis is carried out using the Shuey approximation by considering the Poisson ratio, normal incident, and correction from the Shuey and Aki-Richard equations^{19,20,21)}

$$R(\theta) = R_p + \left(R_p A_0 + \frac{\Delta\sigma}{(1-\sigma)^2} \right) \sin^2 + \frac{1}{2} \frac{\Delta V_p}{V_p} (\tan^2 \theta - \sin^2 \theta) \quad (2)$$

where RP is the normal incident and is the Poisson ratio. Well LAC-12 was selected to carry out the gradient analysis for AVO analysis. Two horizons were picked in the well, approximately at a depth of 2500 and 2500 m. This picking process was based on the log qualitative interpretation underlining the triple combo log and cross-plot result that shows the reservoir potential. Furthermore, by using Eq. 2, we can determine the intercept and gradient volume for creating the AVO attribute. In this research, we used the AVO Scaled Poisson's Ratio Change to search for reservoir potential. This attribute uses the equation below^{22,23)}.

$$R(\theta) = R_p + G \sin^2 \theta \quad (3)$$

$$\text{where, } R_p = \frac{1}{2} \left(\frac{\Delta V_p}{V_p} + \frac{\Delta \rho}{\rho} \right), \quad (4)$$

$$G = R_p \left(D - 2(1 + D) \frac{1-2\sigma}{1-\sigma} \right) + \frac{\Delta \sigma}{(1-\sigma)^2} \quad (5)$$

And

$$D = \frac{\frac{\Delta V_p}{V_p}}{\frac{\Delta V_p}{V_p} + \frac{\Delta \rho}{\rho}} \quad (6)$$

The attribute will be used to support the interpretation of the inversion result qualitatively^{12,24)}. This research will use three post-stack attributes, namely RMS amplitude, sweetness and spectral decomposition. RMS amplitude aims to search for big amplitudes (high or low), which could infer the distribution of lithology. The root mean square amplitude (RMS) is a commonly used technique to

display amplitude values in a specified window of stack data. With RMS amplitude, hydrocarbon indicators can be mapped directly by measuring reflectivity in a zone of interest based on equation (4)²⁵⁾

$$A_{RMS} = \sqrt{\frac{1}{n} \sum_{t=1}^n A(t)^2} \quad (7)$$

The sweetness attribute shows the hydrocarbon-prone area that is indicated by high instantaneous amplitude and low frequency²⁶⁾. Sweetness is calculated by dividing the instantaneous amplitude (amplitude envelope) by the square root of the instantaneous frequency as follows²⁷⁾

$$s(t) = \frac{A(t)}{\sqrt{\omega(t)}} \quad (8)$$

where the instantaneous frequency is represented by $\omega(t)$ and the instantaneous amplitude by $A(t)$.

The last method of interpretation is spectral decomposition, which can be used for two different purposes: low-frequency analysis, which looks for low-frequency anomalies for hydrocarbon exploration, and the RGB attribute, which incorporates three frequency bands—low, mid, and high—to illustrate the structure interpretation. Using a Ricker wavelet and a continuous wavelet transform, spectral decomposition will be performed^{28,29)}. Azimuth, dip, frequency, and other properties can all be subjected to spectral decomposition; however, frequency analysis is the most frequently used. Even when the recorded seismic data has a wavelet overprinting it, narrow beds have distinct frequency expressions. Therefore, if the time domain of the recorded traces is converted to the frequency domain using^{29,30)}.

3. Results and Discussion

3.1. Sensitivity Analysis (Cross plot) Result

Sensitivity analysis was performed using a cross plot between two parameters, with the parameter being the color to distinguish conglomerates around the volcanic rock (extrusive rock and dominantly volcanic tuff). The output is expected to be a cut-off value that the parameters will use to distinguish the desired events. In this study, we analyzed the parameters that will undergo the inversion process, such as Zp (the impedance of P waves), Zs (the impedance of S waves), density, and Vp/Vs. As we can see in Figure 4, we are creating Zp vs. Zs, Vp/Vs vs. Zp, Vp/Vs vs. density, and Vp/Vs vs. Zs using water saturation as the color key, respectively.

As shown in Figure 4.A, P-impedance (Zp) and S-impedance (Zs) do not separate the low-water-saturation sample, suggesting the presence of hydrocarbons and implying conglomeratic lithology. Similarly, in Figure 4.B (Vp/Vs vs. Zp) and Figure 4.D (Vp/Vs vs. Zs), the low-water-saturation sample also remains indistinguishable.

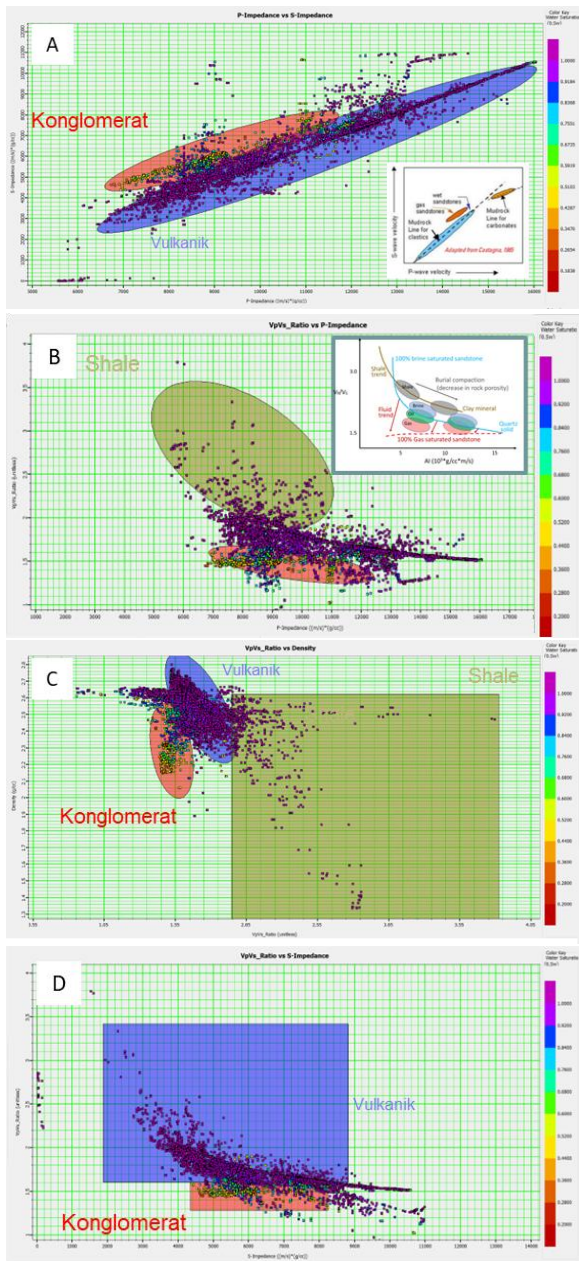


Fig. 4: Sensitivity Analysis between four parameters that will undergo an inversion process. (A) P-impedance vs S-impedance, (B) P-impedance vs V_p/V_s , (C) V_p/V_s vs Density, (D) S-impedance vs V_p/V_s

Throughout the four parameters, V_p/V_s and density (Figure 4.C) are the best parameters that are sensitive enough to distinguish between volcanic rock and conglomerate rock, with cut-off values approximately less than 1.6 for V_p/V_s and less than 2.35 g/cc for density. Other than V_p/V_s and density, the Lambda-rho parameter is also sensitive to separate the conglomerates with a cut-off value of approximately less than 20 GPa*cc/cc.

3.2. Simultaneous Inversion Result

Simultaneous inversion is carried out with input data in the form of initial model inversion parameters (AI, SI, ρ , V_p , V_s , and V_p/V_s), 3D seismic angle gather data, and wavelet

groups consisting of near angle, mid angle, and far angle. The main results of the simultaneous inversion in this study are the cubes of acoustic impedance, shear impedance, density, P and S wave velocity, and V_p/V_s . After creating the inversion parameter cubes, we create the map slices on the horizons of Pre-TAF and the top of the basement. Based on the cross-plot results, three parameters can be used or are sensitive to differentiate between conglomerate and volcanic rock, namely lambda-rho, V_p/V_s , and density (Figure 5.A–5.C). Lambda-rho is applied qualitatively in this study, without fluid substitution analysis, and is interpreted as a supportive elastic parameter rather than a direct fluid indicator (Goodway et al., 1997).

The cut-off values for V_p/V_s , $\lambda\rho$, and density were derived from cross-plot analysis of the available well logs, ensuring that the seismic-based classification is consistent with petrophysical data. In the V_p/V_s parameter, the cut-off value is indicated by the start of the yellow color on the map slice, where there are several locations as shown in the red circle in Figure 5. This is like the lambda-rho parameter, which at nearly the same location has a low incompressibility value of $> 20 \text{ GPa*cc/gram}$ marked with colors ranging from yellow to red indicated by a red circle. Followed by the density that indicated a green color, which shows a density ranging from 2.45 to 2.4 g/cc.

3.3. Seismic Attributes

The sweetness attribute can show a tendency for the location of hydrocarbons, which in Figure 5.E shows a high sweetness value in the LAL-33 well area on the right and the LAC-20 well on the left. Furthermore, the RMS Amplitude attribute displays a high amplitude distribution dominantly located in the south of the study area (Figure 5.D), where there is a high amplitude value in the west of the study area, which can be interpreted as a conglomerate with hydrocarbons. Next, Figure 5.F shows a map slice at a frequency of 10 Hz, which shows several low-frequency effect anomalies characterized by high amplitudes in several places, such as around wells LAL-33 and LAC-20, which are the most dominant, and LAC-12 and LAL-27, which are moderate. This high amplitude shows a low-frequency effect on the presence of fluids, based on the research of Goloshubin³¹⁾ where low frequencies can help identify the presence of hydrocarbons.

RGB attributes are created using frequency data of 20 Hz as low frequency, 40 Hz as mid-frequency, and 60 Hz as high frequency, which are marked in red, green, and blue, respectively. Figure 6 shows the results of the RGB attribute, which can highlight the existence of a structure as marked by the dotted blue circle. Then, because this attribute separates high-frequency data from low-frequency data, it can identify not only major faults but also minor faults.

3.4. AVO Analysis and Attribute Results

The results of the AVO analysis have positive intercept values and negative gradients at the top and bottom picks (Figure 7). At the near-offset, the amplitude still has a positive value. Furthermore, amplitude dimming occurs at the mid offset, and polarity reversal occurs at the far offset at the top reservoir, not at the bottom reservoir, which already has a negative intercept. Then the cross plot between the intercept and gradient shows that the target

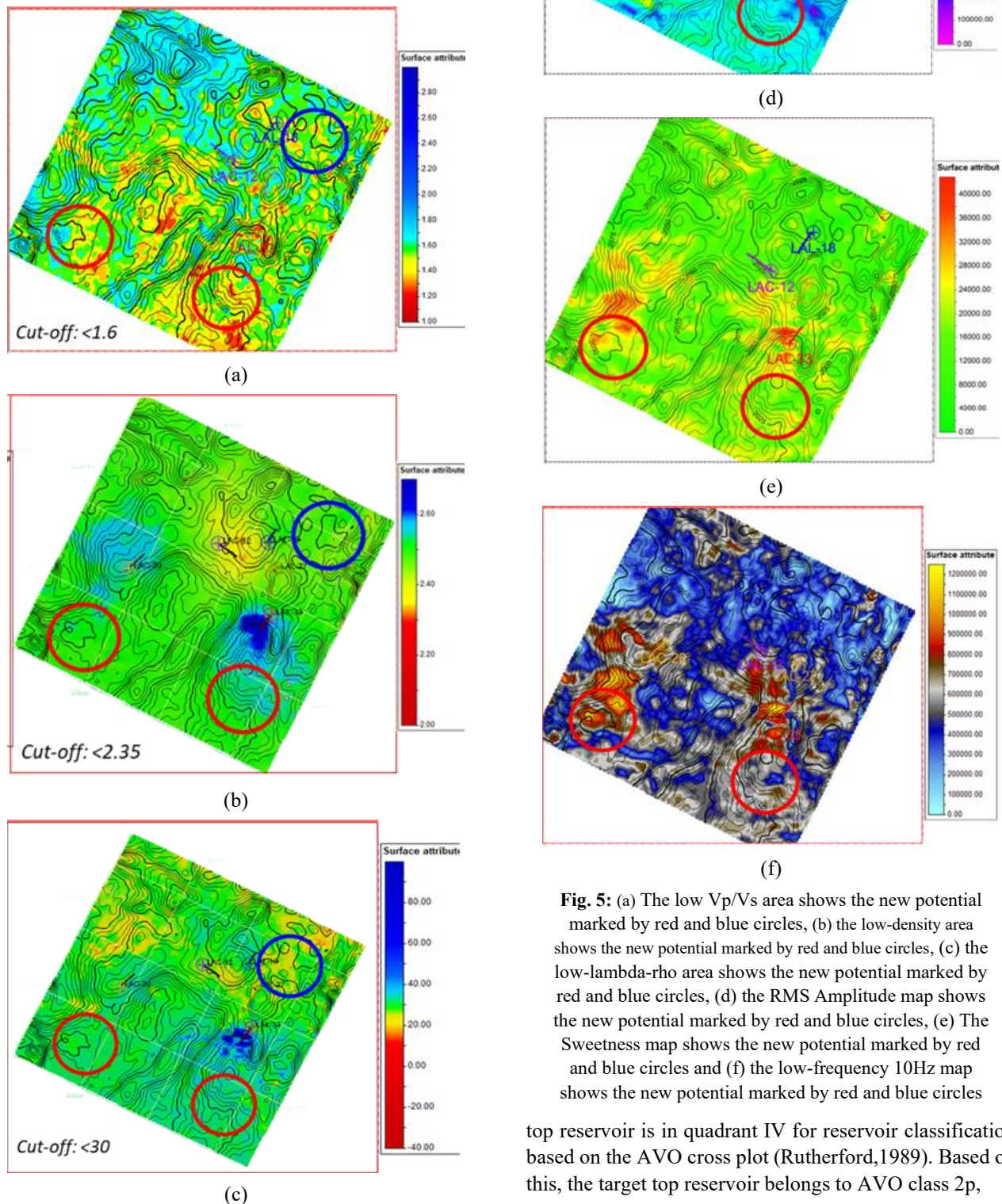


Fig. 5: (a) The low Vp/Vs area shows the new potential marked by red and blue circles, (b) the low-density area shows the new potential marked by red and blue circles, (c) the low-lambda-rho area shows the new potential marked by red and blue circles, (d) the RMS Amplitude map shows the new potential marked by red and blue circles, (e) The Sweetness map shows the new potential marked by red and blue circles and (f) the low-frequency 10Hz map shows the new potential marked by red and blue circles

top reservoir is in quadrant IV for reservoir classification based on the AVO cross plot (Rutherford,1989). Based on this, the target top reservoir belongs to AVO class 2p,

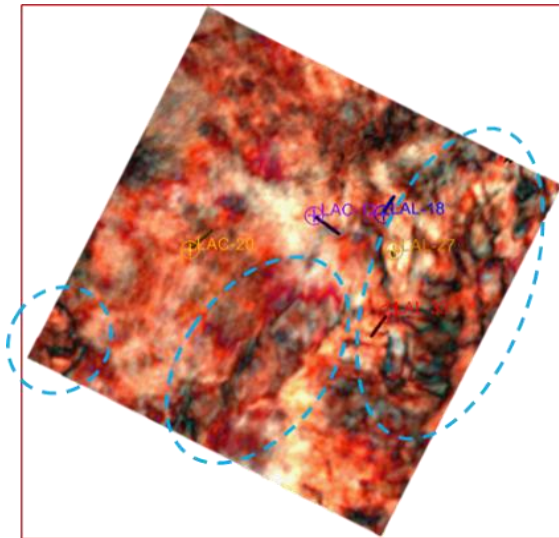


Fig. 6: Determination of the frequency and data used in creating RGB attributes that display several structures. The most noticeable structure is shown by the blue-dotted circle

which is characterized by a positive but near-zero intercept and a negative gradient and is in quadrant IV. The target bottom reservoir belongs to AVO class 2, which is characterized by a negative intercept but near zero, a negative gradient, and is in quadrant III.

The scaled Poisson's ratio change attribute is used to see the gas response, which is characterized by a negative value because the presence of gas will cause the P wave velocity to decrease. Goodway³²⁾ explained that the top reservoir will have a negative value, and the base reservoir will have a positive value. This can be caused by the not-too-high hydrocarbon saturation in the layer, so that the deviation in the mud rock line curve is not too far from the background trend¹⁸⁾.

The cross-section in Figure 8 shows several places that have gas potential. This is shown in the dark red dotted box in the LAL-12 well, which has proven to be hydrocarbon. Then we found a negative top response and a positive bottom in several places, one of which is in the southern part of the LAL-33 well, which is marked with a dark red dotted box. In the qualitative evaluation, the LAL-33 well has no potential when viewed from the log results; this is in line with the results of this attribute, where at the location of the LAL-33 well, no clear negative top and positive bottom were found, which are marked with colored dotted boxes in light blue^{33,34,35)}.

At well LAL-33, amplitude-based attributes such as sweetness and RMS, together with the inversion results, indicated a potential anomaly. However, the subsequent AVO analysis did not show a hydrocarbon-consistent response. This discrepancy highlights the different sensitivities of the methods. This case illustrates the importance of integrating multiple attributes and reinforces that interpretation should not rely solely on a single method.

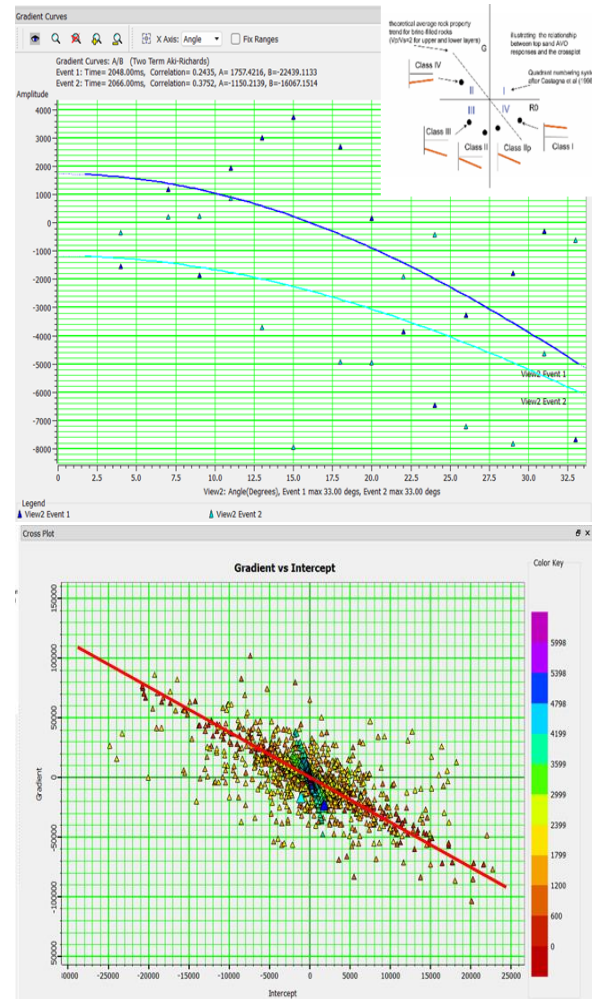


Fig. 7: AVO Analysis with gradient analysis (left) and cross plot between intercepts and gradients. The gradient analysis and cross-plot show that the top of the reservoir is AVO class 2p and the bottom of the reservoir is AVO class 2. The cross plot also showed the distance between the reservoir and the mud rock line is in the middle, suggesting there is a presence of gas and water

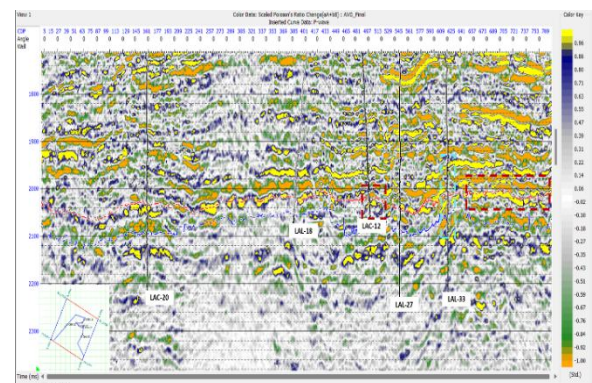


Fig. 8: The seismic cross section on the attribute-scaled Poisson's ratio changes at the arbitrary line. The section shows several potential areas that are indicated by a red dotted box, while this attribute also shows why LAL-33 didn't have gas potential despite previous interpretations using simultaneous inversion and seismic attributes

4. Conclusion

In this study, simultaneous inversion was used to characterize the distribution of conglomerate among volcanic rocks by using several sensitive parameters consisting of V_p/V_s with a cut-off value of <1.6 , density with a cut-off value of <2.35 g/cc, and λ -rho, or incompressibility < 20 Gpa*g/cc. AVO analysis on the LAC-12 well showed that the reservoir in this study was of class IIP AVO type at the top and class II at the base. In addition, the RMS amplitude, sweetness, and spectral decomposition attributes are used in the interpretation of this study, which indicates several potential locations. Then, the RGB attribute is used in the spectral decomposition data to support the interpretation of the structure at the study site. In the end, this attribute is integrated with the inversion parameter and supported by the interpretation of the AVO attribute cross-section, which produces three potential locations in the pre-TAF horizon with a depth of about 2100 ms and spread over the study area marked with the locations of the red and blue circles. These potential location exhibit responses consistent with conglomeratic reservoirs and may represent preliminary geophysical leads. However, they should not be regarded as confirmed prospects, since no quantitative risk assessment were conducted in this study. Further work, including probabilistic risk evaluation, net pay estimation, and volumetric analysis, is necessary to establish the exploration relevance of these locations.

Acknowledgements

This research is supported by Universitas Gadjah Mada to facilitate a partnership with PT. PERTAMINA EP, which provides the data and software necessary for the authors to conduct this research comprehensively.

References

- 1) Noble, R. A., Pratomo, K. H., Nugrahanto, K., Ibrahim, A. M. T., Prasetya, I., Mujahidin, N., W. C. H., & Howes, J. V. C., "Petroleum systems of northwest Java, Indonesia," Proc. Indon. Petrol. Assoc., International Conference on Petroleum Systems of SE Asia and Australasia. (1997).
- 2) Putra, S. D. H., Suryantini, and W. Srigutomo, "Thermal modeling and heat flow density interpretation of the onshore Northwest Java Basin, Indonesia," Geothermal Energy, 4(1) (2016). doi: 10.1186/s40517-016-0052-x.
- 3) M.G. Bishop, "Petroleum systems of the Northwest Java Province, Java, and offshore southeast Sumatra, Indonesia," Reston, VA (2000), doi: 10.3133/ofr9950R.
- 4) Glesko, M., Suria C., and, Sinclair, S., "Basin Evolution of the Ardjuna Rift System and Its Implications For Hydrocarbon Exploration, Offshore Northwest Java, Indonesia," Proc. Indon. Petrol. Assoc., 24th Ann. Conv. (1995).
- 5) Herianto, H., "Determination of Hydrocarbon Zones Using Logging Data Analysis in A Sandstone Reservoir (Case Study: Structure 'TL' Basin North West Java)," Indonesian Journal on Geoscience, 5(3), 251–263 (2018). <https://doi.org/10.17014/ijog.5.3.251-263>
- 6) Aveliansyah, Ponco, P., Triyono, W., Saefullah, U., "Pre-Talang Akar Formation: New Hopes for Hydrocarbon Exploration in the Offshore," Proc. Indon. Petrol. Assoc., 40th Ann. Conv (2016).
- 7) Russell, B. H., "Introduction to Seismic Inversion Method (S. N. Domenico, Ed.)," Society of Exploration Geophysics, 1988 <https://doi.org/10.1190/1.9781560802303>
- 8) Rutherford, S. R., & Williamst, R. H., "Amplitude-versus-offset variations in gas sands," Geophysics, 54(6), 680–688 (1989). <https://doi.org/10.1190/1.1442696>
- 9) Booth, A. D., Emir, E., & Diez, A., "Approximations to seismic AVA responses: Validity and potential in glaciological applications," Geophysics, 81(1), WA1–WA11 (2016). <https://doi.org/10.1190/GEO2015-0187.1>
- 10) Castagna, J. P., & Backus, M. M., "Offset-dependent Reflectivity: Theory and Practice of AVO Analysis (Michael R Cooper, Ed.)." Society of Exploration Geophysics, 1993. <https://doi.org/10.1190/1.9781560802624>
- 11) Russell, B. H., Gray, D., & Hampson, D. P., "Linearized AVO and poroelasticity," Geophysics, 73(3), C19–29, (2011). <https://doi.org/https://doi.org/10.1190/1.3555082>
- 12) Chopra, S., & Marfurt, K. J., "Seismic attributes — A historical perspective". Geophysics, 70(5), 3SO–28SO, (2005). <https://doi.org/10.1190/1.2098670>
- 13) Sarhan, M. A., "The efficiency of seismic attributes to differentiate between massive and non-massive carbonate successions for hydrocarbon exploration activity," NRIAG Journal of Astronomy and Geophysics, 6(2), 311–325, (2017). <https://doi.org/10.1016/j.nrjag.2017.06.003>
- 14) Kriski, L., Muhtar, M. Indah Nursina, I. Suropto Suyatno, H. Heru Prasetijo, and H. Niko Saputra, "De-Risking Exploration Well In A Mature Basin, Jabung Block, South Sumatra Basin: Application of Avo Analysis In A Sub-Unconformity Play," Indonesia Petroleum Association (IPA) (2022).
- 15) Al Muhaidib, A. M., Sen, M. K., & Nafi Toksoz, M., "Integration of geology, rock physics, logs, and pre-stack seismic data for reservoir porosity estimation," AAPG Bulletin, 96(7), 1235–1251 (2012). <https://doi.org/10.1306/01021211083>

- 16) Xu, S., & White, R. E., "A new velocity model for clay-sand mixtures," *Geophysical Prospecting*, 43(1), 91–118, (1995). <https://doi.org/10.1111/j.1365-2478.1995.tb00126.x>
- 17) Hampson D., and B., Russel, "Simultaneous inversion of pre-stack seismic data," CSEG National Convention (2005). doi:10.1190/1.2148008
- 18) Fatti, J. L., Smith, G. C., Vail, P. J., Strauss, P. J., and Levitt, P. R., "Detection of gas in sandstone reservoirs using AVO analysis: A 3-D seismic case history using the Geostack technique", *Geophysics*, 59(9) (1994). <https://doi.org/10.1190/1.1443695>
- 19) Sheriff, R. E., & Geldart, L. P., "Exploration Seismology". Cambridge University Press, 1995. <https://doi.org/10.1017/CBO9781139168359>
- 20) Shuey, R. T., "A simplification of the Zoeppritz equations," *Geophysics*, 50, 1984, p.609-614 (1984). <https://doi.org/10.1190/1.1441936>
- 21) Aki, K., and Richards, P.G., "Quantitative Seismology 2nd edition," University Science Books, 2002.
- 22) Young, R. A., & LoPiccolo, R. D., "A comprehensive AVO classification," *The Leading Edge*, 22(10), 1030–1037 (2003). <https://doi.org/10.1190/1.1623645>
- 23) Bagdassarov, N., "Fundamentals of Rock Physics," Cambridge University Press, 2021. doi: 10.1017/9781108380713.
- 24) Oumarou, S., Mabrouk, D., Tabod, T. C., Marcel, J., Ngos III, S., Essi, J. M. A., & Kamguia, J., "Seismic attributes in reservoir characterization: an overview," *Arabian Journal of Geosciences*, 14(5), 402, (2021). <https://doi.org/10.1007/s12517-021-06626-1>
- 25) Pamungkas, T. D., Nandi, & Ridwana, R., "Conceptual interpretation seismic 3d using rms amplitude and dip-azimuth attribute analysis for identification structure and facies model in physical geographic," *IOP Conference Series: Earth and Environmental Science*, 683(1), 012055, (2021). <https://doi.org/10.1088/1755-1315/683/1/012055>
- 26) Emujakporue, G. O., & Enyenihi, E. E., "Identification of seismic attributes for hydrocarbon prospecting of Akos field, Niger Delta, Nigeria," *SN Applied Sciences*, 2(5), 910, (2020). <https://doi.org/10.1007/s42452-020-2570-1>
- 27) Hart, B. S., "Channel detection in 3-D seismic data sing sweetness," *American Association of Petroleum Geologists Bulletin*, 92(6), 733–742, (2008). <https://doi.org/10.1306/02050807127>
- 28) Maurya, S. P., Singh, N. P., and Singh, K. H., "Seismic Inversion Methods: A Practical Approach," Springer, 2020. doi.org/10.1007/978-3-030-45662-7
- 29) Curia, D., Strecker, U., and Veeken, P., "Anisotropy Analysis of Vaca Muerta Source Rocks and Multicomponent Seismic Inversion, Bandurria Norte Concession, Argentina," First EAGE Conference on Seismic Inversion, 1 – 5 (2020). <https://doi.org/10.3997/2214-4609.202037015>
- 30) Barnes, A., "Handbook of Poststack Seismic Attributes (Vol. 21)," Society of Exploration Geophysicists, 2016. <https://doi.org/10.1190/1.9781560803324>
- 31) Goloshubin, G., Korneev, V., and Vingalov V., "Seismic low-frequency effects from oil-saturated reservoir zones," SEG Technical Program Expanded Abstracts, 1813-1816, 2002. doi:10.1190/1.1815739
- 32) Goodway, B., Suria, C., and Sinclair, S., "Improved AVO Fluid Detection and Lithology Discrimination Using Lamé Petrophysical Parameters; " $\lambda\rho$," " $\mu\rho$," & " λ/μ Fluid Stack", from P and S Inversions," SEG Technical Program Expanded Abstracts, 183–186, (1997). <https://doi.org/10.1190/1.1885795>
- 33) Hampson D., and Russel, B., "Hampson Russell Help System". CGG, Veritas, 2018.
- 34) Ismail, A., Ewida, H. F., . Al-Ibiary, M. G, and Zollo, A., "Application of AVO attributes for gas channels identification, West offshore Nile Delta, Egypt," *Petroleum Research*, 5 (2) 112–123 (2020). doi: 10.1016/j.ptlrs.2020.01.003.
- 35) Gray, D., and F., Anderson, "The application of AVO and inversion to the estimate of rock properties," CSEG Recorder (26) 105-110 (2001). doi: <https://doi.org/10.3997/2214-4609.202037015>